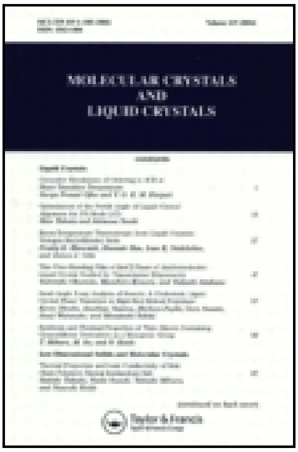

Molecular Crystals and Liquid Crystals
Publication details, including instructions for authors and subscription information:
http://www.tandfonline.com/loi/gmcl20

Liquid Crystalline Behavior of Binary Mixtures of Structurally Dissimilar Mesogens and Nonmesogens

Jayrang S. Dave [a], Purvang D. Patel [a] & Himanshu S. Bhatt [a]

[a] Applied Chemistry Department, Faculty of Technology and Engineering, M. S. University of Baroda, Vadodara, India

Published online: 22 Apr 2013.

Mol. Cryst. Liq. Cryst., Vol. 575: pp. 8–21, 2013

ISSN: 1542-1406 print/1563-5287 online
DOI: 10.1080/15421406.2013.766920

Liquid Crystalline Behavior of Binary Mixtures of Structurally Dissimilar Mesogens and Nonmesogens

JAYRANG S. DAVE,* PURVANG D. PATEL, AND HIMANSHU S. BHATT

Applied Chemistry Department, Faculty of Technology and Engineering, M. S. University of Baroda, Vadodara, India

We have studied eight binary systems comprising three enantiotropic nematogens, namely 4-(4′-n-butyloxybenzoyloxy)phenylazo-4″-fluorobenzene, 4-(4′-n-butyloxybenzo yloxy)benzylidene-4″-fluoro aniline, and 4-(4′-n-heptyloxybenzoyloxy)phenylazo-4″-fl uorobenzene; a monotropic nematogen, viz. 4-(4′-n-dodecyloxybenzoyloxy)napthylazo-4″-fluorobenzene; and three nonmesogens, viz. 4-(4′-n-butyloxy benzoyloxy)benzalde hyde, 4-methoxybenzylidene-4′-chloroaniline, and 4-methoxybenzylidene-4′-toluidine. The central linkage, terminal group, and central ring system of the components have been varied systematically and the effect of these variations has been evaluated on the liquid crystalline properties of the binary mixtures. The mixed mesomorphic properties of these systems are discussed on the basis of their phase diagrams.

Keywords Binary mixtures; emergence; enantiotropic nematic; monotropic nematic; nonmesogen; structurally dissimilar

Introduction

Physical properties of individual mesogens may or may not undergo modifications in their mixtures. Sometimes, the modifications become characteristic, thereby making the study of mixtures important. Earlier studies [1–7] have suggested the formation of mixed mesomorphism by mixing compounds where none, one, or both of them are mesogens. Emergence of the mesophase [8], increase or decrease in the mixed mesomorphic ranges and thermal stabilities, and study of the factors that influence the modifications have received greater attention. The binary mixtures of mesogens have provided better formulations for applications in different field [9].

We have re-reported binary systems of structurally similar and dissimilar mesogens and nonmesogens [10]. Continuing our research in this field, we report here four binary systems consisting of structurally dissimilar mesogens and the study of their effect on mixed mesomorphism, arising due to the differences in structural characteristics of these components.

*Address correspondence to Jayrang S. Dave, Applied Chemistry Department, Faculty of Technology and Engineering, M. S. University of Baroda, Vadodara 390 001, India. Tel.:+91-265-2434188 Ext. 212; Fax: +91-265-2423898. E-mail: jayrangdave@yahoo.com

We have also reported binary systems of mesogens and nonmesogens [11]. Continuing our research in this field, we report here eight binary systems consisting of nonmesogen (A1 = BBB [12], A2 = MBCA, A3 = MBT), monotropic nematogen (A4 = DNFB), and enantiotropic nematogen (B1 = BPFB [13], B2 = BBFA, B3 = HPFB [13]) (Scheme 1).

The binary systems studied are (I) BBB + BPFB, (II) BBB + BBFA, (III) MBCA + BBFA, (IV) MBCA + HPFB, (V) MBT + BBFA, (VI) MBT + HPFB, (VII) DNFB + BPFB, and (VIII) DNFB + BBFA.

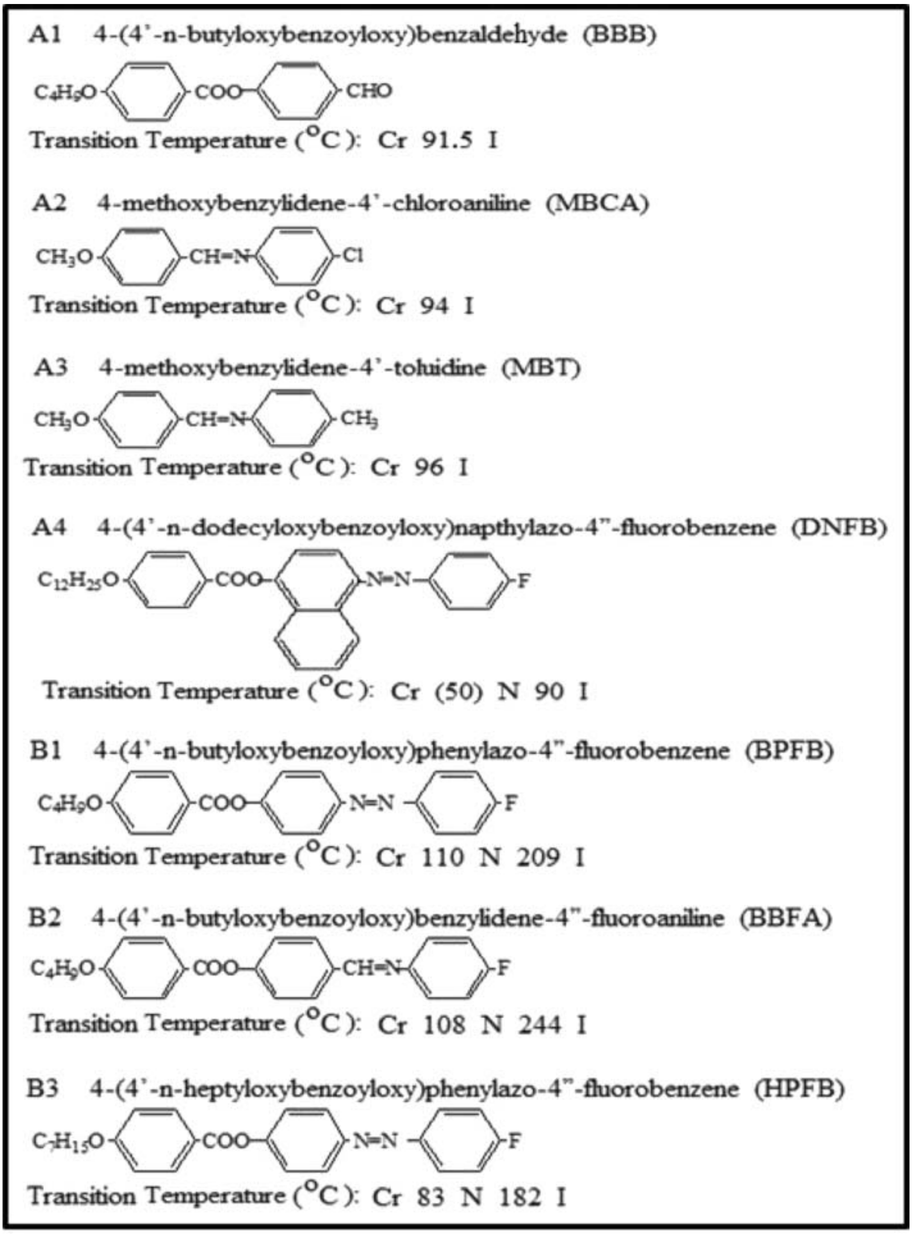

Scheme 1. The structural formula of the components.

Experimental

All the chemicals are of Merck grade and used as received. 4-n-alkoxybenzoicacids and 4-n-alkoxy benzoylchlorides are synthesized by the modified method of Dave and Vora [14]. 4-hydroxy phenylazo-4′-fluorobenzene and 4-hydroxynapthylazo-4′-fluoro benzene are synthesized by the reported method in Ref. [15]. Condensation of (1) 4-hydroxybenzaldehyde with 4-n-butyloxybenzoylchloride, (2) 4-hydroxynapthylazo-4′-fluo robenzene with 4-n-dodecyloxybenzoylchloride, (3) 4-hydroxy phenylazo-4′-fluorobenz ene with 4-n-butyloxybenzoylchloride, and (4) 4-hydroxyphenylazo-4′-fluorobenzene with 4-n-heptyloxybenzoylchloride are done by known methods [16].

4-methoxybenzylidene-4′-choroaniline (A2), 4-methoxybenzylidene-4′-toluidine (A3), and 4-(4′-n-butyloxybenzoyloxy)benzylidene-4″-fluoroaniline (B2) are synthesized by taking equimolar quantities of 4-methoxybenzaldehyde with 4-chloroaniline, 4-methoxybenzaldehyde with 4-toluidine, and 4-(4′-n-butyloxybenzoyloxy)benzaldehyde with 4-fluoroaniline, respectively, in minimum quantity of ethanol with a few drops of glacial acetic acid and refluxing it for a period of 6–8 hours. The product is filtered, dried, and recrystallized from ethanol until constant transition temperatures are obtained. The synthetic route is shown in Scheme 2. Their infrared (IR) spectra are recorded on a Perkin Elmer GX-FTIR:

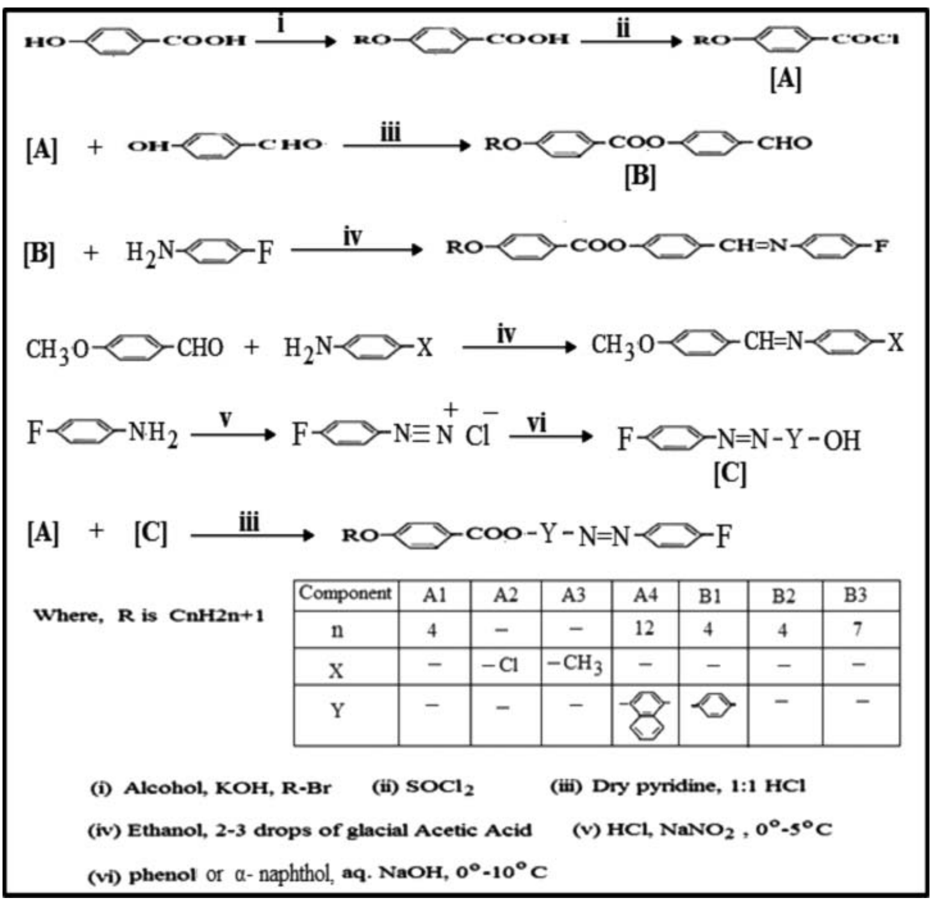

Scheme 2. Synthetic route for components A1, A2, A3, A4, B1, B2, and B3.

Fourier Transform Infrared (Nujol, KBr pellets, cm^{-1}):

Component A1 4-(4′-n-butyloxybenzoyloxy)benzaldehyde (BBB)
2953, 2939, 1729 (ester), 1680 (aldehyde), 1600, 1253, 1066 (ether), 690

Component A2 4-methoxybenzylidene-4′-chloroaniline (MBCA)
2957, 2915, 1602, 1390, 1170 (azomethane), 1255, 1082 (ether), 692

Component A3 4-methoxybenzylidene-4′-toludine (MBT)
2939, 2924, 1608, 1393, 1170 (azomethane), 1255, 1078 (ether), 694

Component A4 4-(4′-n-dodecyloxybenzoyloxy)napthylazo-4′′-fluorobenzene (DNFB)
2950, 2926, 1733 (ester), 1606, 1359, 1170 (azo), 1259, 1064 (ether), 690

Component B1 4-(4′-n-butyloxybenzoyloxy)phenylazo-4′′-fluorobenzene (BPFB)
2958, 2920, 1729 (ester), 1597, 1496, 1389, 1199 (azo), 1258, 1073 (ether), 969, 761, 692.

Component B2 4-(4′-n-butyloxybenzoyloxy)benzylidene-4′′-fluoroanilinne (BBFA)
2955, 2916, 1737 (ester), 1606, 1396, 1170 (azomethane), 1259, 1064 (ether), 694

Component B3 4-(4′-n-heptyloxybenzoyloxy)phenylazo-4′′-fluorobenzene (HPFB)
2959, 2928, 1739 (ester), 1608, 1359, 1174 (azo), 1255, 1062 (ether), 692

Preparation and Study of Binary Mixtures

The components are weighted in known proportions and melted together in fusion tubes. They are thoroughly mixed in their melt to obtain a homogeneous mixture, after which they are cooled. This procedure is repeated three times. The solid obtained is finally ground and used for determining transition temperatures, by using a Leitz laborlux 12 POL polarizing microscope fitted with a Kofler heating stage. Figure 1 shows the photomicrographs of some of the representative mixtures.

Results and Discussion

Binary System I: BBB (A1) + BPFB (B1)

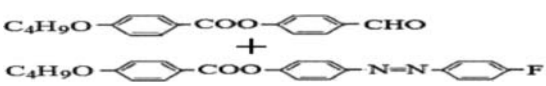

(A1) Cr 91.5 I

(B1) Cr 110 N 209 I

In this system (Table 1, Fig. 2), component A1 is nonmesogen (Cr 91.5 I), whereas B1 is nematogen (Cr 110 N 209 I), showing the nematic mesophase with marble texture. The phase diagram of this system shows that the nematic phase emerges in enantiotropic form by the addition of as low as 10.97 mole% of B1 and continues to be exhibited till the addition of 90.69 mole% of B1. The mixed nematic phase also shows marble texture. As the concentration of B1 increases, the mixed nematic mesophase range increases; eutectic point is obtained at 47°C at 40.25 mole% of B1 and maximum mesophase range of 131°C is observed at 90.69 mole% of B1. In this system, the N–I curve shows rising tendency, with steep increase from 70.10 mole% of B1 and then a fall of 12°C at 100 mole% of B1. Thus, the N–I curve shows nonlinear behavior. Some of the binary mixtures supercool up to about 40°C.

Table 1. Binary system I: BBB (A1) + BPFB (B1)

	Transition temperature (°C)	
Mole% B1	Nematic	Isotropic
0	—	91.5
10.97	58	85
20.92	60	98
30.77	59	118
40.25	47	132
50.60	58	151
60.73	60	151
70.10	80	175
80.46	82	210
90.69	90	221
100	110	209

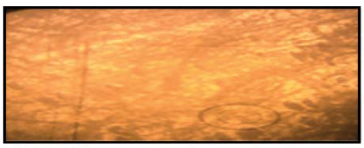

(a) Marble texture of nematic phase Binary system I (39.27 mole%)

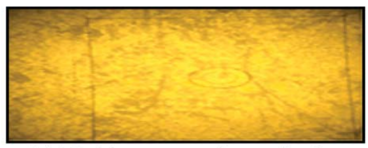

(b) Marble texture of nematic phase Binary system II (59.02 mole%)

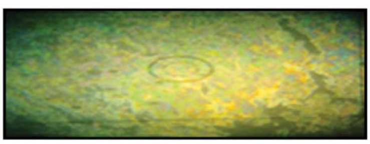

(c) Marble texture of nematic phase Binary system III (69.24 mole%)

(d) Threaded texture of nematic phase Binary system IV (39.75 mole%)

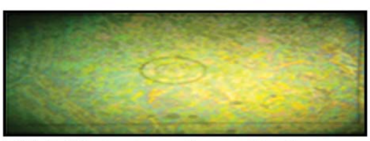

(e) Marble texture of nematic phase Binary system V (79.43 mole%)

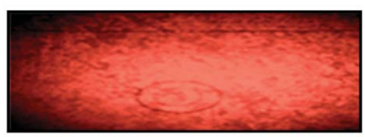

(f) Marble texture of nematic phase Binary system VI (20.51 mole%)

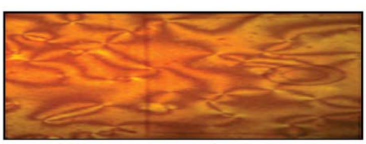

(g) Schlieren texture of nematic phase Binary system VII (69.82 mole%)

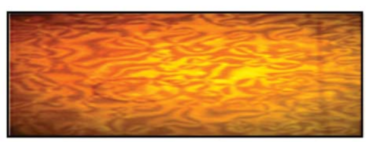

(h) Schlieren texture of nematic phase Binary system VIII (78.48 mole%)

Figure 1. Photomicrographs of the textures of some of the representative mixtures.

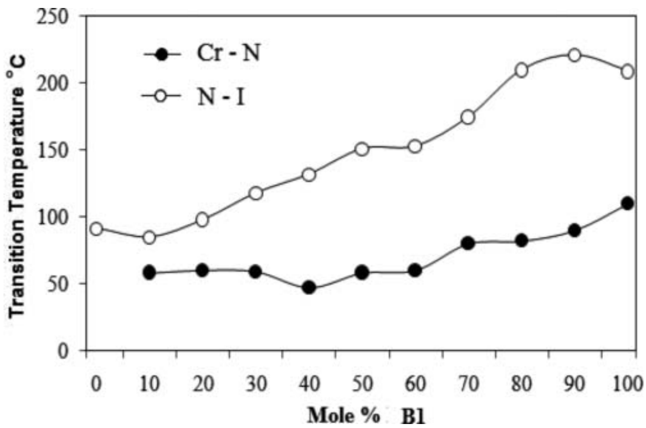

Figure 2. Phase diagram of binary system I: BBB (A1) + BPFB (B1).

Binary System II: BBB (A1) + BBFA (B2)

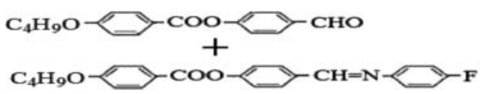

(A1) Cr 91.5 I

(B2) Cr 108 N 244 I

In this system (Table 2, Fig. 3), component A1 is nonmesogen (Cr 91.5 I), whereas B2 is nematogen (Cr 108 N 244 I), showing the nematic mesophase with marble texture. Here also, the nematic phase emerges in enantiotropic form by addition of as low as 10.54 mole% of B2 and continues to be exhibited till the addition of 90.57 mole% of B2. The mixed nematic phase also shows marble texture. As the concentration of B2 increases, the mixed nematic mesophase range increases. Eutectic point is obtained at 65°C at 69.94 mole% and maximum mesophase range of 140°C is observed at 90.57 mole% of B2. In this

Table 2. Binary system II: BBB (A1) + BBFA (B2)

	Transition temperature (°C)	
Mole% B2	Nematic	Isotropic
0	—	91.5
10.54	47	87
19.52	52	105
30.25	50	162
40.98	48	145
49.46	70	150
60.51	80	191
69.94	65	200
80.66	100	224
90.57	105	245
100	108	244

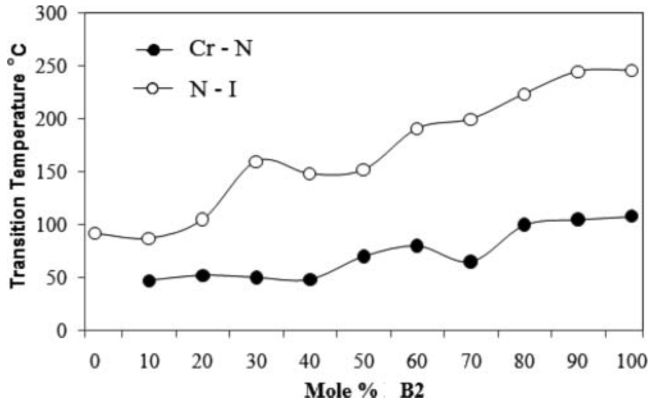

Figure 3. Phase diagram of binary system II: BBB (A1) + BBFA (B2).

system, the N–I curve shows rising tendency, with a jump at 30.25 mole% of B2; thus, the N–I curve shows nonlinear behavior. Some of the binary mixtures supercool up to about 40°C.

Binary System III: MBCA (A2) + BBFA (B2)

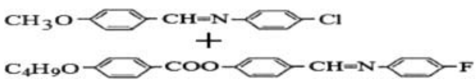

(A2) Cr 94 I

(B2) Cr 108 N 244 I

This system (Table 3, Fig. 4) consists of component A2, which is nonmesogen (Cr 94 I), and component B2, which is nematogen (Cr 108 N 244 I), showing the nematic mesophase with marble texture. The mesogenic characteristic emerges in monotropic form by the

Table 3. Binary system III: MBCA (A2) + BBFA (B2)

	Transition temperature (°C)	
Mole% B2	Nematic	Isotropic
0	—	94
8.93	(79)	80
19.60	(75)	83
28.13	80	89
39.71	71	128
50.17	86	176
59.95	83	157
69.24	91	200
79.57	106	192
90.06	105	206
100	108	244

Note. Values within parentheses indicate monotropic transitions.

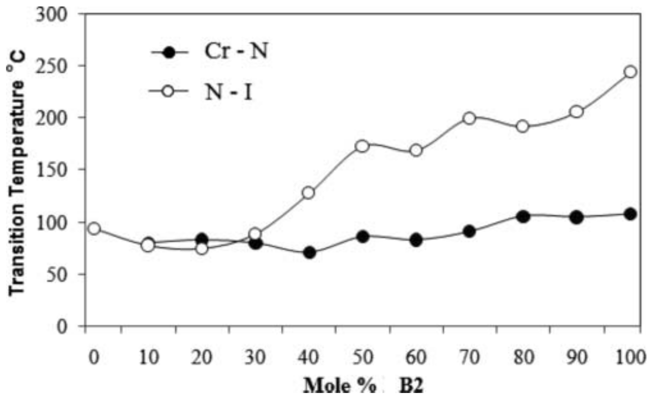

Figure 4. Phase diagram of binary system III: MCBA (A2) + BBFA (B2).

addition of as low as 8.93 mole% of B2, which becomes enantiotropic by addition of 28.13 mole% of B2 and continues to be exhibited till the addition of 90.06 mole% of B2. The mixed nematic phase shows marble texture. As the concentration of B2 increases, the mixed nematic mesophase range increases. Eutectic point is obtained at 71°C at 39.71 mole% of B2 and maximum mesophase range of 109°C is observed at 69.24 mole% of B2. In this system, the N–I curve shows nonlinear behavior with overall rising tendency, with increase in concentration of B2. Some of the binary mixtures supercool up to about 50°C.

Binary System IV: MBCA (A2) + HPFB (B3)

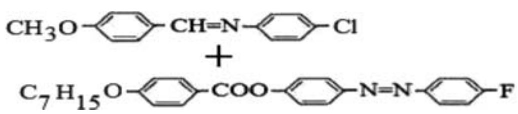

(A2) Cr 94 I

(B3) Cr 83 N 182 I

Table 4. Binary system IV: MBCA (A2) + HPFB (B3)

	Transition temperature (°C)	
Mole% B3	Nematic	Isotropic
0	—	94
9.76	—	90
19.34	(38)	83
29.32	60	86
39.75	64	89
49.77	62	98
59.56	66	92
69.22	50	122
79.48	60	129
89.08	66	136
100	83	182

Note. Values within parentheses indicate monotropic transitions.

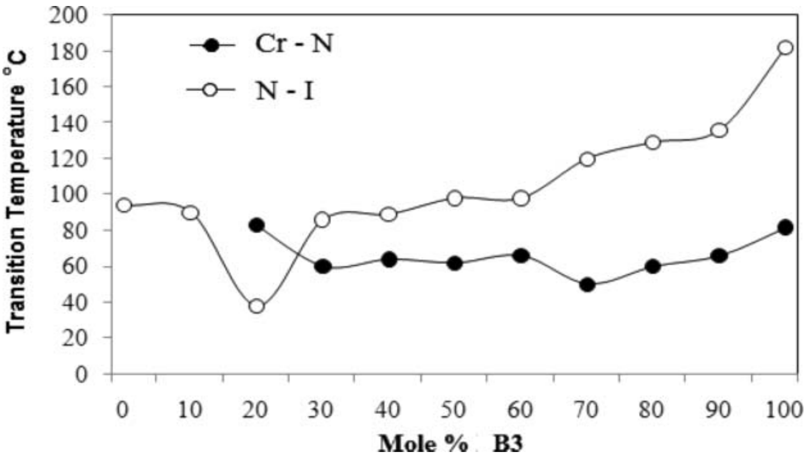

Figure 5. Phase diagram of binary system IV: MBCA (A2) + HPFB (B3).

Phase diagram of this system (Table 4, Fig. 5) shows that the nematic phase emerges as monotropic form by the addition of 19.34 mole% of nematogen B3 (Cr 83 N 182 I) in nonmesogen A2 (Cr 94 I). The monotropic nematic phase is transformed into enantiotropic form by addition of 29.32 mole% of B3 and continues to be exhibited till the addition of 89.08 mole% of B3. The mixed nematic phase shows threaded texture. As the concentration of B3 increases, the mixed nematic mesophase range also increases. Eutectic point is obtained at 50°C at 69.22 mole% of B3 and maximum mesophase range of 72°C is observed at the same concentration. In this system, the N–I curve shows nonlinear behavior, with overall rising tendency with increase in the concentration of B3. Some of the binary mixtures supercool up to about 45°C.

Table 5. Binary system V: MBT (A3) + BBFA (B2)

	Transition temperature (°C)	
Mole% B2	Nematic	Isotropic
0	—	96
9.43	—	78
19.55	(54)	82
29.03	78	111
39.72	75	126
49.80	71	146
59.25	60	169
69.01	80	191
79.43	106	211
89.07	100	226
100	108	244

Note. Values within parentheses indicate monotropic transitions.

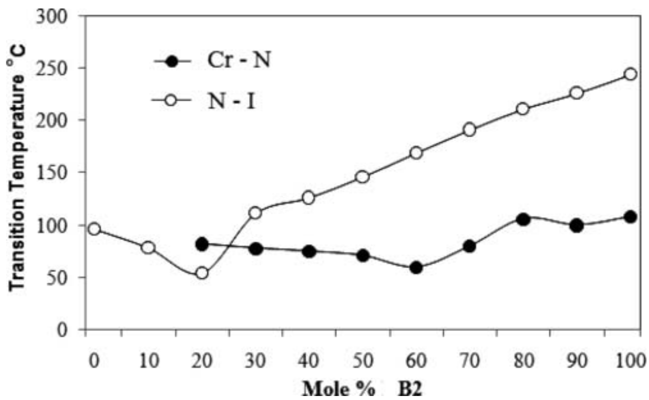

Figure 6. Phase diagram of binary system V: MBT (A3) + BBFA (B2).

Binary System V: MBT (A3) + BBFA (B2)

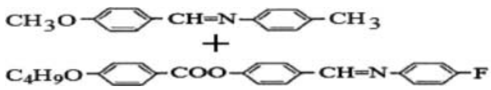

(A3) Cr 96 I

(B2) Cr 108 N 244 I

In this system (Table 5, Fig. 6), component A3 is nonmesogen (Cr 96 I), whereas component B2 is nematogen (Cr 108 N 244 I), showing the nematic mesophase with marble texture. The nonmesogenic component A3 is transformed into monotropic nematogen by the addition of 19.55 mole% of B2. The monotropic nematic phase is transformed into enantiotropic form by the addition of 29.03 mole% of B2 and continues to be exhibited till the addition of 89.07 mole% of B2. The mixed nematic phase also shows marble texture. As the concentration of B2 increases, the mixed nematic mesophase range also increases. Eutectic point is obtained at 60°C at 59.25 mole% of B2 and maximum mesophase range of 126°C is observed at 89.07 mole% of B2. In this system, the N–I curve shows nonlinear behavior, with steep rising tendency with increase in the concentration of B2. Some of the binary mixtures supercool up to about 45°C.

Binary System VI: MBT (A3) + HPFB (B3)

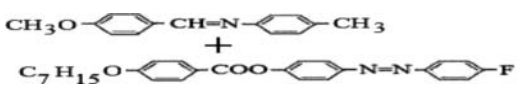

(A3) Cr 96 I

(B3) Cr 83 N 182 I

In this system (Table 6, Fig. 7), component A3 is nonmesogen (Cr 96 I), whereas component B3 is nematogen (Cr 83 N 182 I), showing the nematic mesophase with marble texture. The nonmesogenic A3 is transformed into monotropic nematic phase by the addition of as low as 8.96 mole% of B3. The monotropic nematic phase is transformed into enantiotropic form by the addition of 59.15 mole% of B3 and continues to be exhibited till the addition of 89.84 mole% of B3. The mixed nematic phase also shows marble texture. As the concentration of B3 increases, the mixed nematic mesophase range increases. Eutectic point is obtained at 60°C at 68.83 mole% of B3 and maximum mesophase range of 54°C is also observed at 68.83 mole% of B3. In this system, the N–I curve shows nonlinear behavior, with zig-zag tendency with increase in the concentration of B3. Some of the binary mixtures supercool up to about 50°C.

Table 6. Binary system VI: MBT (A3) + HPFB (B3)

	Transition temperature (°C)	
Mole% B3	Nematic	Isotropic
0	—	96
8.96	—	70
20.51	(50)	79
29.13	80	106
38.77	71	110
50.26	65	100
59.15	73	121
68.83	60	114
79.42	77	126
89.84	79	129
100	83	182

Note. Values within parentheses indicate monotropic transitions.

Binary System –VII: DNFB(A4) + BPFB(B1)

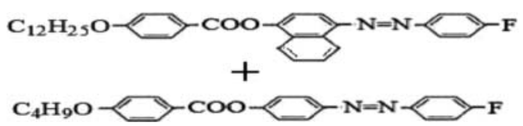

(A4) Cr (50) N 90 I

(B1) Cr 110 N 209 I

In this system (Table 7, Fig. 8), both components A4 and B1 are mesogenic in nature; A4 is monotropic nematogen (Cr (50) N 90 I), whereas B1 is enantiotropic nematogen (Cr 110 N 209 I); the nematic mesophase shows schlieren texture in A4, whereas marble texture in B1. The monotropic nematic phase of A4 is transformed into enantiotropic nematic phase by the addition of as low as 11.06 mole% of B1 and continues to be exhibited till the addition of 90.79 mole% of B1. The mixed nematic phase shows schlieren texture. As the concentration of B1 increases, the mixed nematic mesophase range increases. Eutectic point is obtained at 79°C at 71.40 mole% of B1 and maximum mesophase range of 121°C

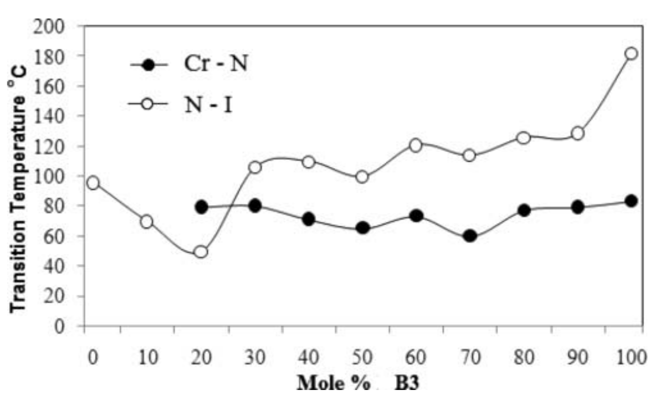

Figure 7. Phase diagram of binary system VI: MBT (A3) + HPFB (B3).

Table 7. Binary system VII: DNFB (A4) + BPFB (B1)

	Transition temperature (°C)	
Mole% B1	Nematic	Isotropic
0	(50)	90
11.06	68	98
20.76	71	106
30.18	75	114
40.43	90	130
50.47	95	145
60.83	96	159
71.40	79	170
80.47	109	184
90.79	89	210
100	110	209

Note. Values within parentheses indicate monotropic transitions.

is observed at 90.79 mole% of B1. In this system, the N–I curve shows rising tendency, with slight increase at 90.79 mole% of B1; thus, the N–I curve shows nonlinear behavior. Some of the binary mixtures supercool up to about 50°C.

Binary System VIII: DNFB (A4) + BBFA (B2)

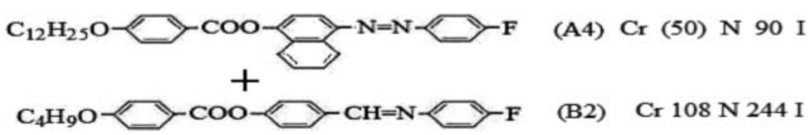

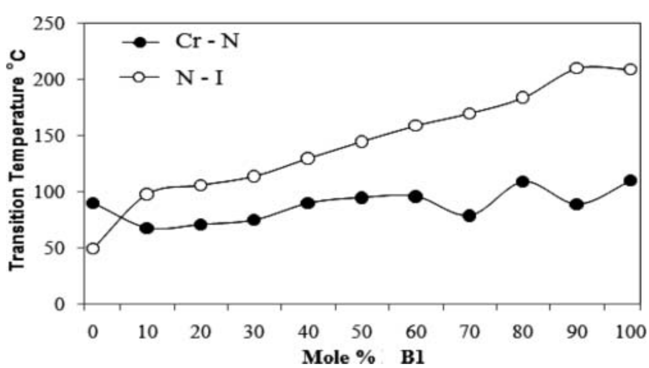

Figure 8. Phase diagram of binary system VII: DNFB (A4) + BPFB (B1).

Table 8. Binary system VIII: DNFB (A4) + BBFA (B2)

	Transition temperature (°C)	
Mole% B2	Nematic	Isotropic
0	(50)	90
10.92	64	89
21.52	66	86
30.78	82	104
40.85	90	118
51.27	92	118
60.44	88	135
70.78	106	173
80.16	99	180
90.94	110	225
100	108	244

Note. Values within parentheses indicate monotropic transitions.

In this system (Table 8, Fig. 9), both components A4 and B2 are mesogenic in nature; A4 is monotropic nematogen (Cr (50) N 90 I), whereas component B2 is enantiotropic nematogen (Cr 108 N 244 I); the nematic mesophase shows schlieren texture in A4, whereas marble texture in B2. The monotropic nematic phase of A4 is transformed into enantiotropic nematic phase by the addition of as low as 10.92 mole% of B2 and continues to be exhibited till the addition of 90.94 mole% of B2. The mixed nematic phase also shows schlieren texture. As the concentration of B2 increases, the mixed nematic mesophase range increases. No eutectic point is obtained and maximum mesophase range of 81°C is observed at 80.16 mole% of B2. In this system, the N–I curve shows rising tendency, with steep rise from 80.16 mole% of B2; thus, the N–I curve shows nonlinear behavior. Some of the binary mixtures supercool up to about 50°C.

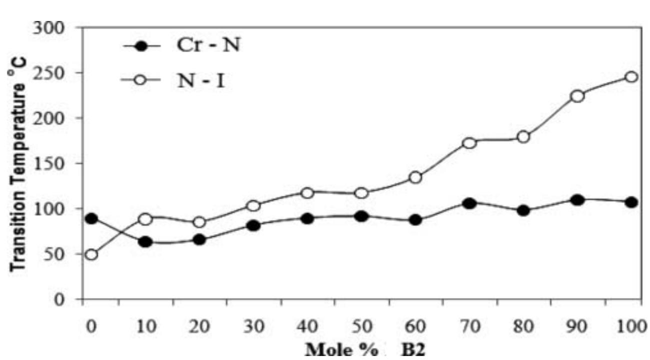

Figure 9. Phase diagram of binary system VIII: DNFB (A4) + BBFA (B2).

Conclusion

All the eight binary systems studied show nonlinear behavior in the N–I curve. This may be due to the fact that all of these binary systems consist of two structurally dissimilar components [17,18]. It is observed that all the binary mixtures exhibit good mixed mesophase range, which is more than the mesophase range of individual components. In the binary systems with the nonmesogen as one of the components, the nematic phase emerges either in monotropic or in enantiotropic form with the addition of as low as 10 to 20 mole% of the nonmesogenic component in the mixture.

Acknowledgments

The authors are thankful to Prof. P.T. Deota, Head, Applied Chemistry Department, Faculty of Technology and Engineering, M. S. University of Baroda, Vadodara, India, for providing laboratory facilities and encouragement.

References

[1] Dave, J. S., & Vasanth, K. L. (1966). *Mol. Cryst. Liq. Cryst.*, *2*, 125–133.
[2] Dave, J. S., Patel, P. R., & Vasanth, K. L. (1969). *Mol. Cryst. Liq. Cryst.*, *8*, 93–100.
[3] Dave, J. S., Menon, M. R., & Patel, P. R. (2003). *Mol. Cryst. Liq. Cryst.*, *392*, 83–95.
[4] Vora, R. A., Gupta, R., & Patel, K. (1991). *Mol. Cryst. Liq. Cryst.*, *209*, 251–263.
[5] Prajapati, A. K., Patel, N. S., & Lad, V. G. (2000). *Mol. Cryst. Liq. Cryst.*, *348*, 41–51.
[6] Vora, R. A. & Rajput, S. J. (1991). *Mol. Cryst. Liq. Cryst.*, *209*, 265–277.
[7] Govindaiah, T. N., Nagappa, Sathyanarayana, P. M., Mahadeva, J., & Sreepad, H. R. (2011). *Mol. Cryst. Liq. Cryst.*, *548*, 55–60.
[8] Lohar, J. M., & Dave, J. S. (1983). *Mol. Cryst. Liq. Cryst.*, *103*, 181–192.
[9] Hird, M., Goodby, J. W., & Toyne, K. J. (2001). *Mol. Cryst. Liq. Cryst.*, *360*, 1–15.
[10] Dave, J. S., Menon, M. R., & Patel, P. R. (2002). *Proc. Indian Acad. Sci.*, *114*(3), 213–221.
[11] Dave, J. S., & Menon, M. R. (1997). *J. Indian Chem. Soc.*, *74*, 809.
[12] Dave, J. S., & Kurian, G. (1975). *J. Physique*, *36*, C1-403-C1-407.
[13] Dave, J. S., Upasani, C. B., & Patel, P. D. (2010). *Mol. Cryst. Liq. Cryst.*, *533*, 73–81.
[14] Dave, J. S., & Vora, R. A. (1970). Photochemical and Thermal stability Studies on a Liquid Crystal Mixture of Cyanobiphenyls. In: J. F. Johnson & R. S. Porter (Eds.), *Liquid Crystals and Ordered Fluids*, Plenum Press: New York, p. 477.
[15] (1989). B. S. Furniss, A. J. Hannford, P. W. G. Smith, & A. R. Tatchell (Eds.). (1989), Aliphatic Compounds. *Vogel's Textbook of Practical Organic Chemistry* (4th ed.), Singapore: Longman Singapore, pp. 563–649.
[16] (1989). B. S. Furniss, A. J. Hannford, P. W. G. Smith, & A. R. Tatchell (Eds.). (1989), Aliphatic Compounds. *Vogel's Textbook of Practical Organic Chemistry* (4th ed.), Singapore: Longman Singapore, pp. 697–698.
[17] Gupta, R., & Vora, R. A. (1984). *Mol. Cryst. Liq. Cryst.*, *106*, 147–159.
[18] Dave, J. S., Menon, M. R., & Patel, P. R. (2001). *Mol. Cryst. Liq. Cryst.*, *365*, 581–591.